Endoscope Manipulator for Trans-nasal Neurosurgery, Optimized for and Compatible to Vertical Field Open MRI

Yoshihiko Koseki[1], Toshikatsu Washio[1],
Kiyoyuki Chinzei[1,2], and Hiroshi Iseki[2,3]

[1] National Institute of Advanced Industrial Science and Technology, 1-2 Namiki, Tsukuba, Ibaraki 305-8564, Japan
koseki@ni.aist.go.jp
http://unit.aist.go.jp/humanbiomed/surgical/
[2] Dept. of Neurosurgery, Neurological Institute, Tokyo Women's Medical University,
[3] Field of Advanced Techno-surgery, Graduate School of Medicine, Tokyo Women's Medical University

Abstract. This paper preliminarily reports the robotic system working inside the gantry of vertical field Open MRI. This manipulator is new in terms of the application to vertical field Open MRI, cost effectiveness, accuracy and stiffness sufficient for endoscope manipulation. The endoscope manipulation for trans-nasal neurosurgery under MR-guidance was selected as the sample task. The endoscope operation in MR-gantry might provide the surgeon(s) with real-time feedback of MR image to endoscopic image and the reverse. This facilitates the comprehensive understanding, because MRI compensates the vision lost through narrow opening of keyhole surgery with global view. So this surgery is a good motivation for combination of MRI and robotic systems. In this paper, the design and implementation are presented and preliminary test shows good MR-compatibility, accuracy and stiffness.

1 Introduction

The merits of MRI (Magnetic Resonance Imaging) are not limited to visualization behind the surface anatomy but also excellent soft tissue discrimination, functional imaging, and non X-ray exposure. Its intra-operative usage can make so-called keyhole surgery safer and effective[1]. Because MRI can compensate the limited view from the narrow opening, and can distinguish the residual tumor from normal tissues. For such usage, some types of widely open MRI have been provided recently.

Many researchers have proposed that the combination of tomography and numerically controlled robot potentially improves the performance of keyhole surgery[2,3]. The robot can position tools and devices referring to precise 3D coordinate of tomography. The technical drawbacks of MRI are that the most conventional materials and devices affect and are affected by the strong and

T. Dohi and R. Kikinis (Eds.): MICCAI 2002, LNCS 2488, pp. 114–121, 2002.

precise magnet[4]. Because of clinical advantages, an MR-compatible robotics has been requested however.

An MR-compatible manipulator was firstly proposed by Masamune to assist needle insertion for stereo-tactic neurosurgery under closed gantry MRI[5]. Kaiser also proposed one for breast cancer[6]. The closed gantry MR scanners generally have better magnetic field properties and are widely used, but have less accessibility to patient. The accessibility to patient must be secured for emergencies during scanning, so the operation inside gantry must be as simple as needle insertion.

We have also investigated the MR-compatibility of mechanical parts and have summarized MR-compatible techniques[7]. Firstly, we developed one prototype for horizontal field Open MRI[8]. This type of MRI is vertically open enough for the surgeon to stand by the patient and to perform the operation inside gantry. In this case, the manipulator is requested not to occupy the surgeon's space nearby the patient.

On the other hand, the vertical field Open MRI is vertically so narrow that the surgeon(s) doesn't stand by the patient while the patient is inside gantry. The hand-works must be done outside and on demand of MR imaging the patient is carried in. This method is clinically and commercially reasonable because a lot of conventional apparatus can be available in many situations. However, a manipulator needs work inside the gantry instead of surgeon.

In case of vertical field Open MRI, the space around the patient remains unoccupied and a manipulator can be closed to the deep inside gantry. This is advantageous in terms of stiffness and precision of the manipulator but disadvantageous in terms of MR-compatibility.

Accordingly, the vertically small shaped prototype was newly designed and implemented for vertical field Open MRI. The prototype is installed to imaging area and has good performance of precision and stiffness. Our continuing studies have revealed that magnetically not ideal parts can be used according to the distance from the imaging area. The cutback of excessively fine MR-compatibility can reduce the cost.

To determine the detailed specifications, an endoscope manipulation of trans-nasal neurosurgery was selected as a sample application. Because the importance of intra-operative MRI is high but almost hand-works have to be performed outside gantry and imaging is not frequent.

2 Design and Implementation

2.1 Scenario

The trans-nasal neurosurgery is one of the most typical keyhole surgeries, where the surgeon(s) approach the pituitary tumor behind sphenoid through the narrow nasal cavity[9]. The surgeon spends the most time on making an approach through sphenoid and resection of the tumor.

The global view and good contrast of soft tissue of MRI are helpful to avoid trauma to critical structures of brain and remove the residual tumor. The real-

time feedback of MRI to endoscopic image and the reverse will enhance the performance and safety of trans-nasal neurosurgery. Although the surgeon cannot hold, pan, or tilt the endoscope stably in vertically narrow MR-gantry, a robotic system can do.

The greater part of this surgery is done in the fringe field and the patient and bed are carried into the gantry on demand of intra-operative MRI. The manipulator should be embedded on the bed for easy carrying in/out. The endoscope should be inserted and removed outside of gantry because the back of endoscope is blocked by the upper magnet while the patient is inside.

2.2 System Requirements

The prototype was designed for Hitachi's AIRIS-II (Hitachi Medical Corp., Tokyo, Japan), whose magnets are 1400[mm] in diameter and are 430[mm] open vertically.

2 DOF (Degree of Freedom) of rotational motions are required for pan and tilt. 2 DOF of translational motions are required for positioning. One DOF around endoscope might be required for potential future usage of angled endoscope but currently not installed.

2.3 Implementation

Previously, MR-compatibility has been applied uniformly. The materials such as titanium and MC Nylon, which are highly compatible, but expensive and weak. Our pretests led that the magnetic effect is inverse proportional to the distance and proportional to the volume. This time incompatible materials and parts were used according to their distance from imaging area and their amount. This enables the stiffness to be improved and the cost to be reduced. The guidelines was set as shown in Table 1.

Fig. 1 shows the mechanism and coordinate system. A rotational 5-bar linkage mechanism was adopted for 2 DOF of translational motions. The reasons are that the actuators are set on distant and immobile points, and the planar parallel mechanism is vertically small compared to a serial mechanism because driving units are arranged in the same plane in parallel. The endoscope is panned around an axis away from the actuator with a parallelogram. This mechanism enabled the actuator distant from imaging area. The endoscope is tilted with the rotation of the parallelogram.

All axes were driven by non-magnetic ultrasonic motors, USR60-S3N (Shinsei Kogyo Corp., Tokyo, Japan) via strain wave gears and hand clutches. Normal strain wave gears, CSF-17 (Harmonic Drive Systems Inc., Tokyo Japan) were used for axis 1 & 2 and low-magnetic ones (custom-made by Harmonic Drive Systems) are used for axis 3 & 4. The strain wave gears reduce the velocity of motors to safe level. The hand clutches can switch from motor drive to manual operation for emergency.

Rotary encoder units, VR-050M&SR-050M (5000P/R, Canon Inc., Tokyo Japan) and potentiometers, JC22E (Nidec Copal Electronics Corp., Tokyo,

Table 1. Zone control of MR-compatibility

	Zone	Guideline	Compatible Materials & Devices
I	Neighborhood of Imaging Area (Within a radius of 300[mm])	Non-magnetic Materials, No Electrical Components	Ti, MC-Nylon, Ceramic Bearing
II	Fringe of Imaging Area (Without a radius of 300[mm])	A Small Amount of Low-Magnetic Materials Electrical Components	Al, SUS304, Low-Magnetic Harmonic Drive, Ultrasonic Motor, Potentio-meter, Rotary Encoder
III	Fringe of Magnet (Without a radius of 700[mm])	A Small Amount of Ferromagnetic	Harmonic Drive, Normal Bearing

The guideline of outer zone includes those of inner zones.

Japan) were installed for precise incremental measurement and absolute measurement of axes respectively. The motor unit and sensors are connected in parallel to axis via parallelogram so the sensors follow the axial motion while the clutch is open. The electrical signals of rotary encoder are optically transmitted to the outside of operation room. Fig. 2 shows the prototype deployed in a dummy of Hitachi's AIRIS-II with a human phantom.

3 Experiments

3.1 Accuracy Test

The accuracy and repeatability of this prototype were tested. Five, 3, and 3 points were selected for X-Y coordinate, axis 3 and 4, respectively. The manipulator moved to each point 20 times on random path. The displacement was measured with two CCD laser micrometers (VG-035/300, KEYENCE, Osaka, Japan). The rotational displacements were indirectly measured by measuring translational displacement of different two points. Table 2 shows ideal positions calculated by kinematics, averages, and standard deviation of measured position.

The accuracy and repeatability were totally good for endoscope positioning. The calibration of mechanical parameters of 5-bar linkage mechanism will improve the accuracy in X- and Y-axes. The error in axis-3 & 4 are relatively large considering of its effect on the tip of 100[mm] endoscope. The error is mainly due to backlash because the error of single path was very small. The pretests revealed that the frictions of these axes increased backlash. As is similar to stiffness, minor changes are necessary.

3.2 Stiffness Test

The major elasticity of this prototype was tested. Up to 20[N] (2.0[kgf]) force was applied on one point close to, and the other point distant from the origin

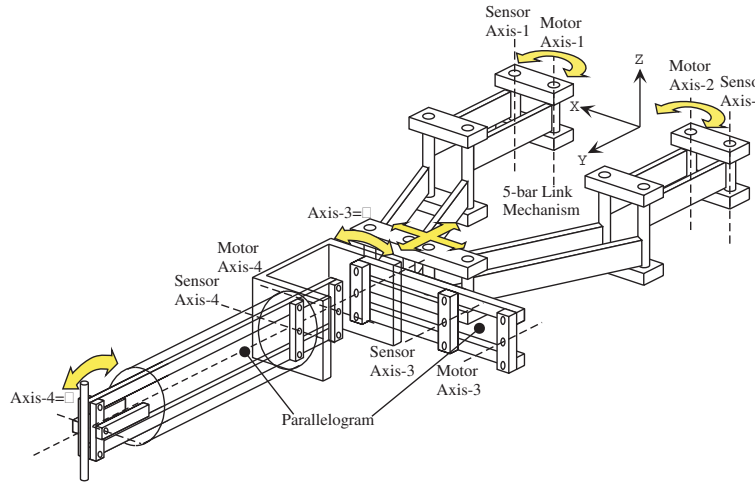

Fig. 1. Mechanism of MR-compatible endoscope manipulator prototype

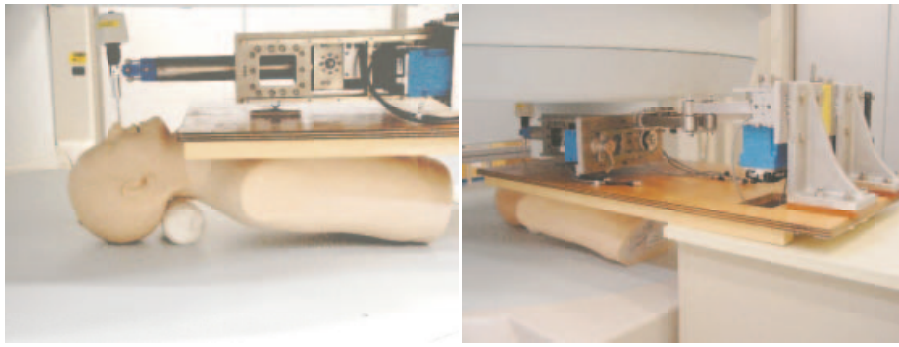

Fig. 2. Prototype of MR-compatible endoscope manipulator in dummy MR gantry

of end-plate, in each direction. The displacements were measured similarly as accuracy test. The coordinate and axes are shown in Fig. 1 and θ_x, θ_y, and θ_z are the rotation around X-, Y-, and Z-axis, respectively. Table 3 shows the elasticity and backlash in positive and negative direction of X, Y, Z θ_x, θ_y, and θ_z.

The elasticity in X-axis was large. The axis 4 was supported by open sided structure (See Fig. 1). The offset of θ_x was also large. Some weak parts were used for knockdown structure around the axis-4. A minor change in mechanism will improve these weaknesses. The stiffness in other directions were excellent.

3.3 MR-Compatibility Test

MRI's Effect to Manipulator. The MR-compatibility of this prototype was tested by real Hitachi's AIRIS-II in Intelligent Operating Room in Tokyo

Table 2. Accuracy & repeatability test

Direction	Ideal	Real Average	STDV
(X, Y)	(0.00, 0.00)	(-, -)	(0.03, 0.02)
([mm], [mm])	(0.00, 5.11)	(0.04, 5.13)	(0.03, 0.01)
	(0.00,-5.34)	(0.05,-5.40)	(0.03, 0.01)
	(7.43,-0.09)	(7.47,-0.03)	(0.02, 0.01)
	(-7.43,-0.09)	(-7.38,-0.20)	(0.02, 0.01)
Axis 3	0.00	-	0.01
[Deg]	5.40	5.40	0.02
	-5.40	-5.38	0.02
Axis 4	0.00	-	0.03
[Deg]	5.40	5.44	0.03
	-5.40	-5.41	0.03

STDV: standard deviation

Table 3. Major elasticity of the prototype

Direction	Pos. [m/N] ([mm/kgf])	Neg. [m/N] ([mm/kgf])	offset [m] ([mm])
x	1.28×10^{-4} (1.28)	1.33×10^{-4} (1.33)	$\pm 0.22 \times 10^{-3}$ ($\pm$0.22)
y	0.07×10^{-4} (0.07)	0.09×10^{-4} (0.09)	$\pm 0.05 \times 10^{-3}$ ($\pm$0.05)
z	0.19×10^{-4} (0.19)	0.24×10^{-4} (0.24])	$\pm 0.03 \times 10^{-3}$ ($\pm$0.03)
Direction	Pos. [Deg/N·m] ([Deg/kgf·cm])	Neg. [Deg/N·m] ([Deg/kgf·cm])	offset [Deg]
θ_x	0.73 (0.073)	0.75 (0.075)	$\pm$1.42
θ_y	0.46 (0.046)	0.54 (0.054)	$\pm$0.66
θ_z	0.25 (0.025)	0.25 (0.025)	$\pm$0.05

Women's Medical University. The manipulator was scanned with spin echo and gradient echo sequence. The followings were confirmed while the manipulator was hard-wired and set on regular position at a standstill.

1. The manipulator was not attracted by the magnet.
2. No heat or noise occurred.
3. The ultrasonic motors worked regularly.
4. The counts of rotary encoders did not change.
5. The noise of potentio-meters was slightly increased at the beginning of scanning.
6. The status of limit switches did not change.
7. The status of emergency switches did not change.

Manipulator's Effect to MRI. The prototype's effect to the images was examined. $1.0l$ aqueous solution of $_2$ 1.8×10^{-4} mol/l NiCl and 0.1% NaCl was imaged as a phantom. The intensity of magnetic field was 0.3 Tesla, and other parameters were TE/TR=20/100[ms], bandwidth=30kHz, Flip Angle=30.0[Deg]. The spin echo image, gradient image, and spectrum of MR on the following conditions were obtained. The 3rd condition is just an auxiliary experiment because the endoscope needs not be operated while MR scanning.

1. The prototype was not installed to the gantry. Only phantom.
2. The prototype was installed to the gantry and hard-wired.
3. The prototype was actuated with the repeat of acceleration and deceleration.

Fig. 3 shows gradient echo MR images on these 3 conditions. Fig. 3 also shows the difference image between condition 1 and 2. Table 4 shows the signal-to-noise ratio (S/N ratio) and half width of MR spectrum. The S/N ratio is the ratio of the mean value of the phantom to the standard deviation of the air. The half width of MR spectrum corresponds to the sharpness of magnetic resonance and indicates the distortion of image. If the magnetic field is distorted, the resonance will be dull.

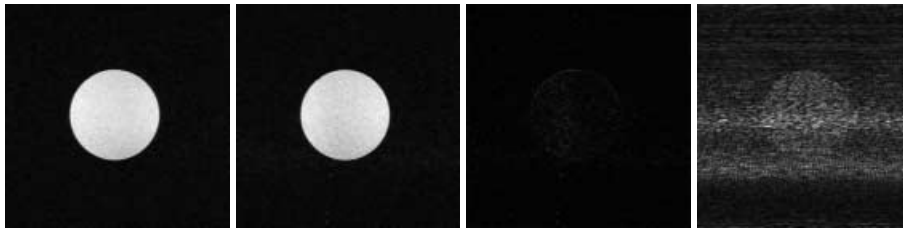

(a) (b) (c) (d)

Fig. 3. Gradient echo MR images of phantom, (a)only a phantom, (b)the manipulator is deployed, (c)the difference image between (a) and (b), (d) the manipulator is actuated

Table 4. Signal to noise ratio and half width of phantom's MR spectrum

Condition	S/N Ratio		Half Width	
	SE	GRE	SE	GRE
Only Phantom	216.7	61.2	33.0	36.1
Manipulator Deployed	208.0	66.4	36.9	37.7
Manipulator Actuated	14.4	11.9	36.1	38.8

The difference images (Fig. 3(c)) led that the manipulator's effect on MRI was negligible. S/N ratio and half width also indicated that no noise or distortion was caused by manipulator as long as the motor was inactive. The actuator caused large noise on MR scanning, however. Assume that the endoscope focuses one area imaged by MRI, the endoscope manipulator needs not move while MR scanning. So this noise doesn't cause trouble.

4 Conclusion

The robotic system working inside the gantry of vertical field Open MRI was studied in this paper. The design and implementation were discussed and the

pre-clinical evaluation of our first prototype like, accuracy test, stiffness and MR-compatibility were reported.

The technical significances of this paper are

1. A manipulator was specially designed for vertical field Open MRI, which is vertically narrow.
2. The zone control reduces the cost and improves the accuracy and stiffness remaining the MR-compatibility.

The clinical significances are

1. This manipulator system enables real-time feedback of MR image to endoscopic image and the reverse.
2. The combination of MRI and endoscope enhances the performance and safety of keyhole surgery.

The pre-clinical evaluations led that some minor modifications are necessary.

References

1. Pergolizzi R.S., et.al.: Intra-Operative MR Guidance During Trans-Sphenoidal Pituitary Resection: Preliminary Results. J. of Magnetic Resonance Imaging, **13** (2001) 136–141
2. Burckhardt C.W., Flury P., Glauser D.: Stereotactic Brain Surgery. IEEE Engineering in Medicine and Biology Magazine, **14(3)**, (1195) 314–317
3. Kwoh Y.S., Hou J., Jonckheere E., Hayati S.: A Robot with Improved Absolute Positioning Accuracy for CT Guided Stereotactic Brain Surgery. IEEE tran. on Biomedical Engineering, **35(2)**(1988), 153–160
4. Jolesz F.A, et al.: Compatible instrumentation for intraoperative MRI: Expanding resources. JMRI, **8(1)** (1998) 8–11
5. Masamune K., Kobayashi E., Masutani Y., Suzuki M., Dohi T., Iseki H., Takakura K.: Development of an MRI-compatible needle insertion manipulator for stereotactic neurosurgery. Journal of Image Guided Surgery. **1(4)** (1995) 242–248
6. Kaiser W.A., Fischer H., Vagner J., Selig M.: Robotic system for Biopsy and Therapy in a high-field whole-body Magnetic-Resonance-Tomograph. Proc. Intl. Soc. Mag. Reson. Med. **8** (2000), 411
7. Chinzei K., Kikinis R., Jolesz F.A.: MR Compatibility of Mechatronic Devices: Design Criteria. Proc. of MICCAI'99, (1999) 1020–1031
8. Chinzei K., Hata N., Jolesz F.A., Kikinis R.: MR Compatible Surgical Assist Robot System Integration and Preliminary Feasibility Study. Proc. of MICCAI 2000 921–930
9. Griffith H.B., Veerapen R.: A direct transnasal approach to the sphenoid sinus. Technical note. J Neurosurgery **66** (1987) 140–142.